Magnetic energy-based understanding the mechanism of magnetothermal anisotropy for macroscopically continuous film of assembled Fe_3O_4 nanoparticles

Fengguo Fan, Jia Liu, Jianfei Sun, Siyu Ma, Peng Wang, and Ning Gu

Citation: AIP Advances **7**, 085109 (2017);
View online: https://doi.org/10.1063/1.4991059
View Table of Contents: http://aip.scitation.org/toc/adv/7/8
Published by the American Institute of Physics

Magnetic energy-based understanding the mechanism of magnetothermal anisotropy for macroscopically continuous film of assembled Fe_3O_4 nanoparticles

Fengguo Fan,[1,2] Jia Liu,[3] Jianfei Sun,[1,a] Siyu Ma,[1] Peng Wang,[1] and Ning Gu[1,a]

[1]*State Key Laboratory of Bioelectronics, Jiangsu Key Laboratory of Biomaterial and Device, School of Biological Science and Medical Engineering, Southeast University, Dingjiaqiao 87, Nanjing 210009, China*

[2]*Shangqiu Normal University, Department of Physics, Shangqiu, Henan 476000, China*

[3]*State Key Laboratory for Mechanical Behavior of Materials, School of Materials Science and Engineering, Xi'an Jiaotong University, Xi'an, Shanxi 710049, China*

(Received 20 June 2017; accepted 9 August 2017; published online 21 August 2017)

The magnetothermal effect in two-dimensional assemblies of magnetic nanoparticles has played an increasingly important role in many biomedical applications. However, determining the mechanism of magnetothermal conversion of the assembled magnetic nanoparticles remains challenging. Here, a macroscopically continuous film assembled of Fe_3O_4 nanoparticles was used as a model for investigation utilizing both simulation and experimentation. The magnetic energy simulated by micro-magnetics can explain the phenomenon in which the assembled film of Fe_3O_4 nanoparticles showed the magnetothermal anisotropy in the presence of an alternating magnetic field. Here, the magnetic interaction between nanoparticles is proposed to play an important role in this process. Furthermore, it was discovered that there is a common behaviour of magnetic moments for the macroscopically continuous nanogranular film and a bulk magnet, which can be exploited to manipulate the magnetothermal effect of nanomaterials. [http://dx.doi.org/10.1063/1.4991059]

INTRODUCTION

Recently, *in vivo* thermal effect have attracted increasing interests from biomedical researchers, as they can be used in hyperthermia,[1–3] controllable drug release,[4,5] self-driven micro-robots[6–8] and so on. Because of their good biocompatibility and ease of remote manipulation by an external field, magnetic nanoparticles are considered as promising building blocks for biomaterials and biodevices *in vivo*.[9–11] Here, it should be mentioned that Ferumxytol which major composition is the iron oxide nanoparticles, is the only inorganic nanodrug approved by FDA to be used in clinic. Thus, the magnetothermal performance of iron oxide nanoparticles, including Fe_3O_4 nanoparticles and γ-Fe_2O_3 nanoparticles will be even more important for the clinic application than that of the other magnetic nanomaterials. With the expanding development of nanomedicine, the application of iron oxide nanoparticles have been expanded from MRI contrast agent into novel scaffolds for tissue engineering. In this case, the nanoparticles are often aggregated together, such as a surface coating film. Although the magnetothermal mechanism of free-floating magnetic nanoparticles has seemed exposited,[12,13] the thermogenesis of assembled nanoparticles remains unclear in the presence of an alternating magnetic field. Here, the interaction between nanoparticles plays a critical role in the magnetothermal conversion.[14] For instance, it has been reported that one-dimensional assemblies of magnetic nanospheres showed a transition of collective magnetism from isotropic superparamagnetism into

[a]Corresponding Email: sunzaghi@seu.edu.cn, guning@seu.edu.cn

weak anisotropic ferromagnetism so that the thermogenesis of the assemblies can be flexibly tuned by alteration of the orientation in the presence of an alternating magnetic field.[15,16] Moreover, it was discovered that a macroscopically continuous film of magnetic nanoparticles that was fabricated by layer-by-layer assembly, also exhibited the similar behaviour.[17,18] However, the anisotropic magnetothermal effect here was dependent upon the level of assembly. This case prompted our research on the dynamics of magnetic moments for a macroscopically continuous film assembled of magnetic nanoparticles.[9,12]

Here, a macroscopically continuous film of Fe_3O_4 nanoparticles was used as a model. The film was fabricated by the layer-by-layer (LBL) assembly method. The employment of Fe_3O_4 nanoparticles mainly resulted from two causes. For one thing, the Fe_3O_4 nanoparticles were the precursors of γ-Fe_2O_3 nanoparticles. The latter can be obtained by oxidization of the former. Both owned the similar magnetic property and biocompatibility. For another, the Fe_3O_4 nanoparticles in our experiments were free of surface coatings, which were stabilized by outward hydroxylation. It was found that the Fe_3O_4 nanoparticles were more stable than the γ-Fe_2O_3 nanoparticles in suspension and the surface charging was more facile to regulate, which was more suitable for he LBL assembly. The magnetic free energy of the LBL-assembled film of nanoparticles was simulated with the OOMMF (Object Oriented Micromagnetic Framework) Program which is theoretically based on the Landau Lifshitz-Gilbert (LLG) equation.[19–22] As seen in the simulation, the magnetic couplings between nanoparticles was a crucial factor determining the emergence of anisotropic thermogenesis for the LBL-assembled film of nanoparticles in the presence of an alternating magnetic field, which can qualitatively explain the experimental results. Moreover, as seen from the simulation, there was a somewhat common behavior of magnetization in the LBL-assembled film of nanoparticles and a disk-like bulk magnet. If there was no internal magnetization inside, the disk-like bulk magnet showed similar magnetothermal anisotropy with the LBL-assembled film of nanoparticles. If there was an internal magnetization inside over the alternating magnetic field in strength, the disk-like bulk magnet showed the opposite case. This phenomenon was confirmed experimentally. Our results will enhance knowledge of the magnetothermogenesis mechanism for magnetic nanomaterials and provided a novel strategy to control the collective magnetothermal effect of magnetic nanoparticles by modulating the couplings between building units.

RESULTS AND DISCUSSIONS

In our experiments, the Fe_3O_4 nanoparticles were synthesized by the classical co-precipitation method, and the morphology is shown in Figure 1a. The Dynamic Light Scattering (DLS) size and the ζ potential are shown in the supplementary material, Fig. S1. The macroscopically continuous film of Fe_3O_4 nanoparticles was fabricated by the LBL assembly method, the process of which is schematically shown in Figure 1b. A photograph and the detailed local characterization of the fabricated film are shown in Figure 1c and d, respectively. SEM-based energy dispersive spectrometer analysis of nanoparticles was shown in supplementary material (Fig. S2a), showing the composition of materials was mainly Fe and O. The powder sample and the LBL-assembled film of nanoparticles were characterized by X-ray diffraction (XRD) to determine the phase composition (supplementary material, Fig. S2b). Compared with the data in literatures,[23–25] the composition of as-synthesized nanoparticles was Fe_3O_4. Moreover, The XRD peaks of powder sample and LBL-assembled film exhibited little alteration so that the LBL assembly was incapable of influencing the phase composition. One advantage of LBL assembly is that the assembly level can be controlled by the layers. More layers lead to a more compact, uniform and regular film. The cross-sectional image of Figure 1c was shown in the supplementary material, Fig. S2c, seen from which the thickness was approximately 210nm. This result was in accordance with the number of assembled layers and size of nanoparticles (20layers and 10nm, respectively). The thermogenic measurement of the LBL-assembled film in the presence of an alternating magnetic field confirmed our previous results (supplementary material, Fig. S3). The 20-layered film exhibited an obvious anisotropy of thermogenesis with alteration of orientation. Furthermore, the anisotropy was dependent upon the assembly level. The thermogenic curves of the LBL-assembled films with various numbers of layers are shown in Fig 2a–d. As can be seen in the experimental results, the 10-layered assembled film of Fe_3O_4 nanoparticles showed

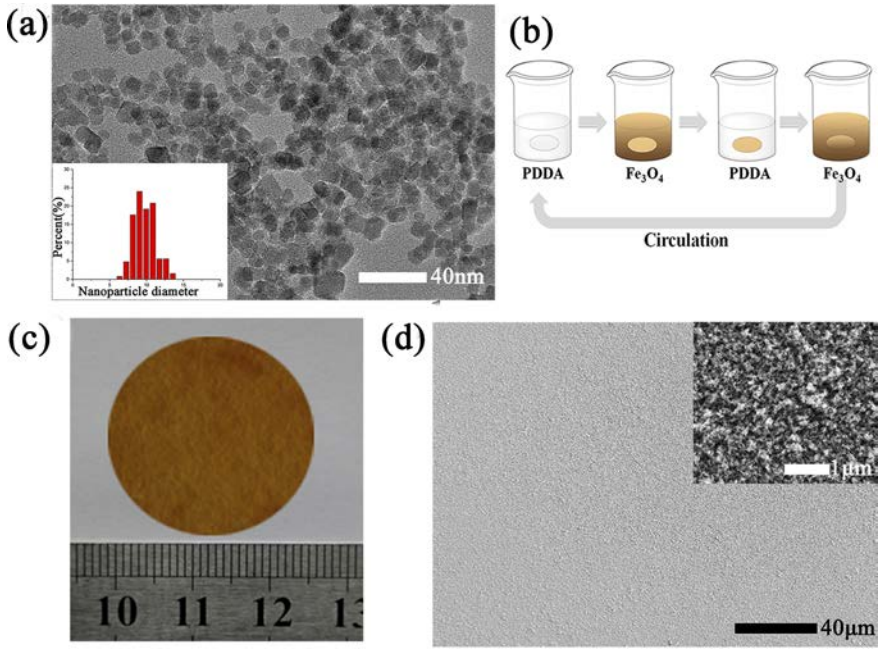

FIG. 1. a) TEM image of synthesized colloidal Fe_3O_4 nanoparticles. Inset: Size distribution of nanoparticles in (a). b) A schematic process of LBL assemble of nanoparticles on a glass substrate. c) Macroscopic picture of the LBL-assembled film. d) Scanning electron microscope (SEM) image of the LBL-assembled film. Inset: SEM image of an LBL-assembled film at high magnification.

little anisotropy. This is because the arrangement of nanoparticles is too sparse. For the 20-layered assembled film, the anisotropy turned was obvious. Furthermore, the thermogenic curves of 30° and 60° approached to the minimal thermogenic curve (90°) for the 20-layered film while they approached to the maximal case (0°) for the 40-layered film.

During the magnetothermal conversion, the energy of the alternating magnetic field is actually dissipated to do work on the magnetic moments of nanoparticles. Here, the Landau-Lifshitz-Gilbert (LLG) equation can be used to describe the dynamics of magnetic moments, where the magnetic Gibb's free energy will be converted into thermal energy. Because the compact, uniform and regular LBL-assembled film of nanoparticles can exhibited some of the properties of bulk materials,[26] the LBL-assembled film of Fe_3O_4 nanoparticles here was considered to be a continuous medium. The alteration of magnetic moments versus time and orientation, simulated by the OOMMF program are shown in the supplementary material, Fig. S4a-f, respectively. The magnetic moments changed periodically with oscillation of the applied magnetic fields in an orientation from the center to the surroundings. Here, the total energy of the magnetic film was called magnetic Gibb's free energy, which included the anisotropy energy, the exchange energy, the magentostatic energy and the Zeeman energy. The magnetic Gibb's free energy of the film was numerically calculated for various relative directions relative to the alternating magnetic field (Figure 3a), which exhibited a high correlation with the heating temperature of the 20-layered film of Fe_3O_4 nanoparticles (Figure 3b). The linear correlation coefficient was 0.99. This result means that the thermogenesis of the LBL-assembled film of Fe_3O_4 nanoparticles in the presence of an alternating magnetic field was highly dependent upon the magnetic Gibb's free energy of the film. For the compact, uniform and regular assembled film of nanoparticles, the thermogenesis of the nano-granular film can be theoretically considered as that of a continuous magnetic medium. Based on the further simulation of the anisotropy energy and the magnetostatic energy, it was inferred that the alteration of the magnetic Gibb's free energy primarily resulted from the dipole interaction between the magnetic nanoparticles (Figure 3c, d). The simulation of Zeeman energy also reflected the fact that the magnetization of nano-granular film was reduced in the presence of external magnetic field with the orientation ranging from 0° into 90° (Figure 3e). The demagnetization field reduced the internal magnetic field of the nanoparticles because of the effect

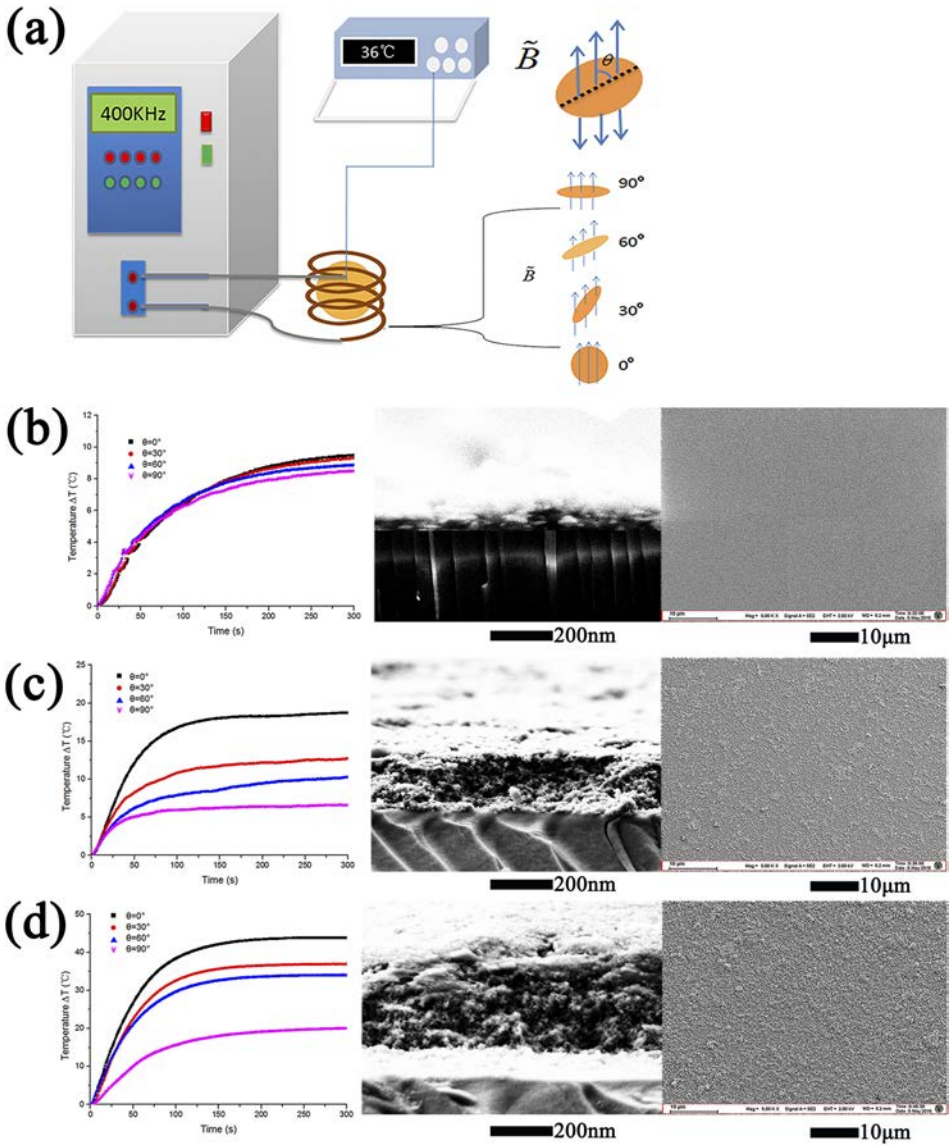

FIG. 2. a) A schematic diagram is designed for magnetothermal measurement under alternating magnetic field (400 KHz). b) The magnetothermal measurement of a 10 layer LBL-assembled nanoparticles film with angle of 0°, 30°, 60°, and 90°, the cross-sectional and SEM. c) The magnetothermal measurement of a 20 layer LBL-assembled nanoparticles film, the cross-sectional and SEM. d) The magnetothermal measurement of a 40 layer LBL-assembled nanoparticles film, the cross-sectional and SEM.

of magnetostatic energy so that the magnetic moments will use more energy to reverse the external field to generate more heat.[27,28] Thus, the LBL-assembled film of Fe_3O_4 nanoparticles exhibited an anisotropic thermogenesis depending on the relative direction of the alternating magnetic field.

Next, we employed the OOMMF program to simulate the Gibb's free energy of magnetic systems composed of 2, 4 and 9 particles in the presence of an alternating magnetic field, respectively. The different number of nanoparticles can partially represent the different assembly levels. The simulated results are shown in Figure 4 and are accordant with the experimental results. It is shown that for a dimer of nanoparticles, the magnetic Gibb's free energy showed little difference with the alteration of the relative direction to the alternating magnetic field. However, for the tetramer of nanoparticles, the magnetic Gibb's free energy showed an obvious difference with the alteration of the relative direction of the alternating magnetic field and the simulated curves of 30° and 60° were close to that of 0°. For the nanomer of nanoparticles, the Gibb's free energy also showed the anisotropy

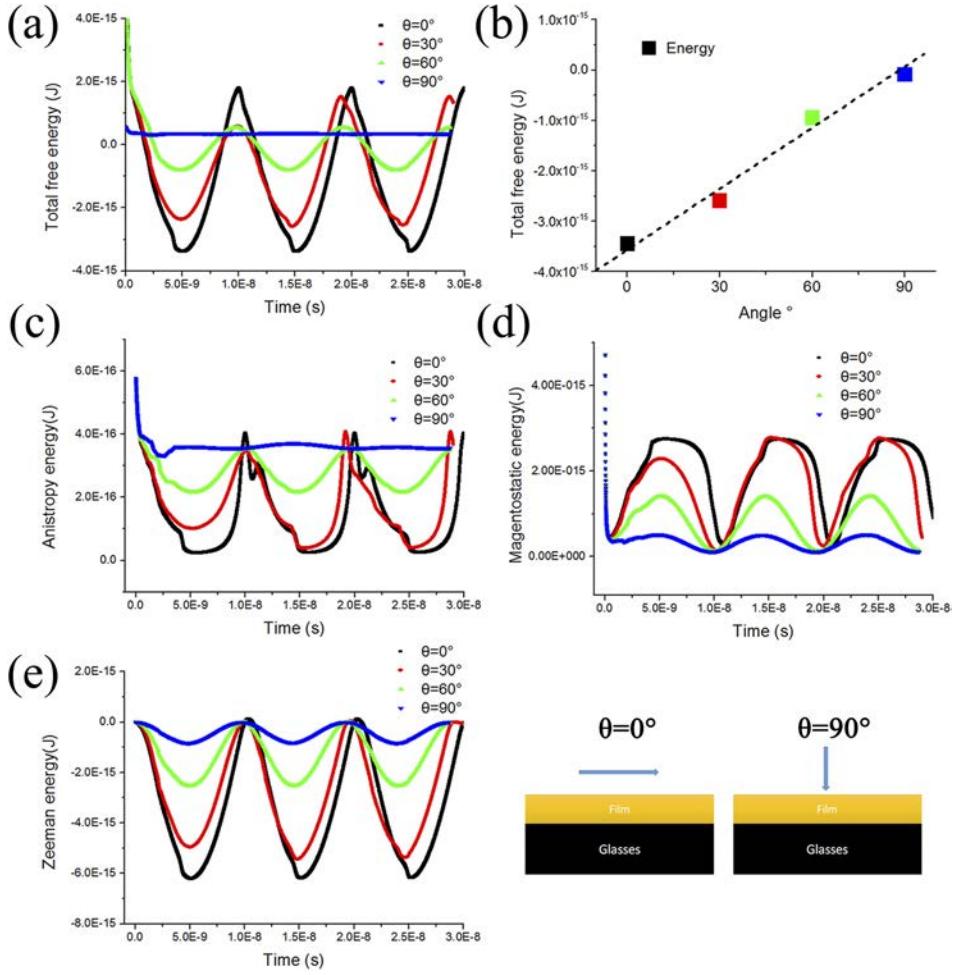

FIG. 3. a) The Gibb's total free energy of the films is simulated, including different angles between the film and the applied alternating magnetic field. b) The correlation between the heating temperature and the angle of the alternating magnetic field. c) The anisotropy energy changes in different directions. d) The magnetostatic energy changes in different directions. e) The Zeeman energy changes in different directions.

and the simulated curves of 30° and 60° were close to that of 90°. This confirmed the validity of the experimental phenomenon. We further studied the influence of different exchange constant between nanoparticles on the magnetic Gibb's free energy. The results for the tetramer of particles are shown in Figure 5. The energy difference among different orientations was obviously augmented with an increase in exchange constant between particles. The simulated results for the nanomer of particles also showed an identical case (supplementary material, Fig. S5). Thus the magnetothermal anisotropy of the assembled magnetic nanoparticles should result from the enhanced interaction between nanoparticles with an increase in number of assembled layers. For only the few layers, the nanoparticles are dispersively arranged, so that the interaction between particles is relatively weak. In this case, the magnetic energy of multi-particles system would be identical for different orientations in the presence of an alternating magnetic field. With an increase in the number of assembled layers, the film of nanoparticles becomes compact. The interaction between nanoparticles is therefore reinforced. Here, the magnetic Gibb's free energy for 0° was significantly greater than that for 90° so that the anisotropy emerged.

Based on the analysis above, the collective magnetothermal effect for the LBL-assembled magnetic nanoparticles should be the sum of that for individual nanoparticles when the nanoparticles are dispersively arranged. However, when the interaction between nanoparticles was adequately strong, the collective magnetothermal property increasingly approached that of a continuous macroscopic

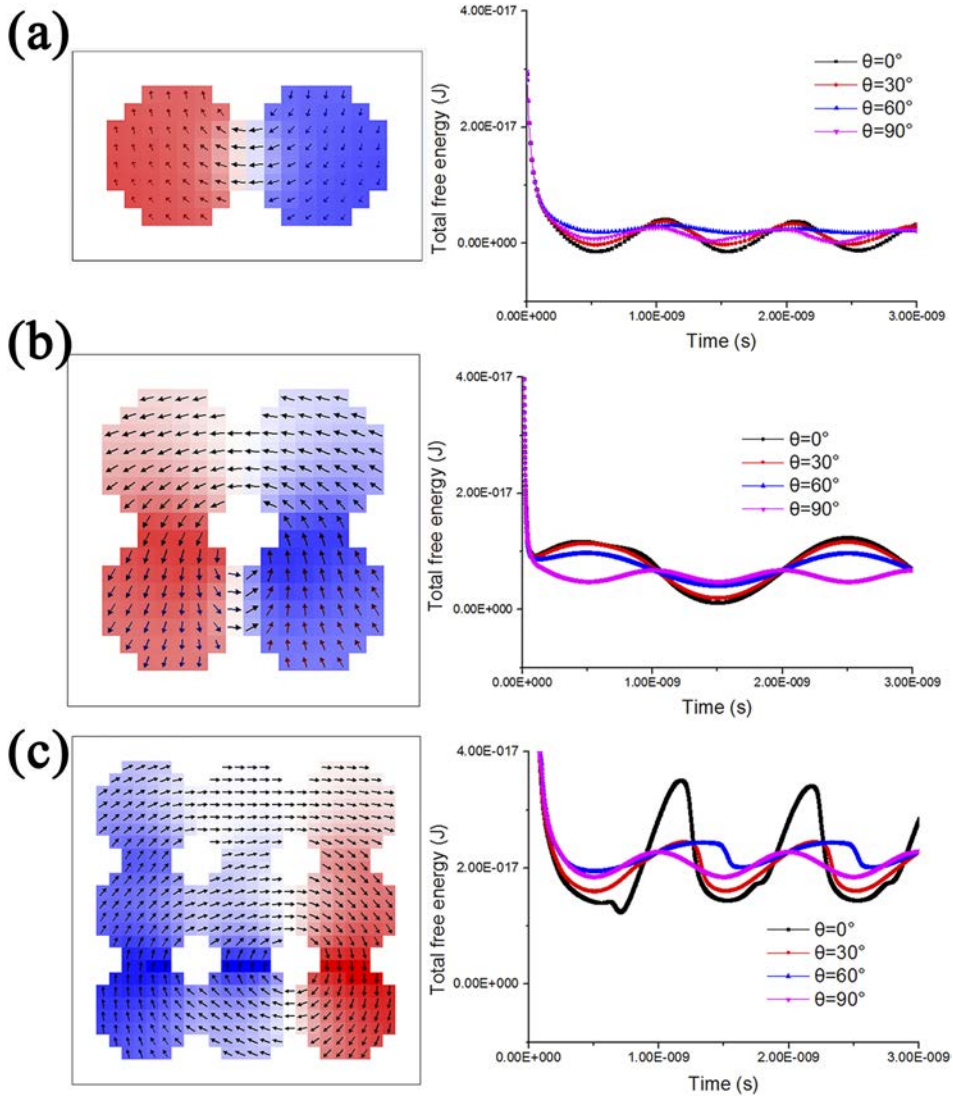

FIG. 4. a) The Gibb's total free energy of two nanoparticles is simulated, including different angle between the film and the applied alternating magnetic field. b) The Gibb's total free energy for four nanoparticles is simulated, including different angle between the film and the applied alternating magnetic field. c) The Gibb's total free energy of nine nanoparticles is simulated, including different angle between the film and the applied alternating magnetic field.

medium. Because there is often residual magnetization inside a magnet, we investigated the effect of inside residual magnetization inside upon the magnetothermal anisotropy. It was discovered with simulation that the residual magnetization inside can reverse the anisotropy of the magnetic Gibb's free energy with respect to different orientations of the alternating magnetic field. The intensity of the alternating magnetic field was set at 20mT and that of the residual magnetization inside was varied from 0 to 60mT. The simulated results are shown in Figure 6a–e. When the intensity of inside residual magnetization was less than 20mT, the magnetic Gibb's free energy in the nearly horizontal direction (60° and 90°) played an insignificant role. However, when the intensity of the inside residual magnetization inside was greater than 20mT, the magnetic Gibb's free energy in the horizontal direction showed a significant variation. This result indicated that the magnetic film will yield the increasing heat in the horizontal direction, even exceeding that in the perpendicular direction, so that the anisotropy will be reversed.

We are incapable of controlling the residual magnetization inside the assemblies of magnetic nanoparticles. However, we employed a disk-like bulk magnet to mimic the granular film. Here,

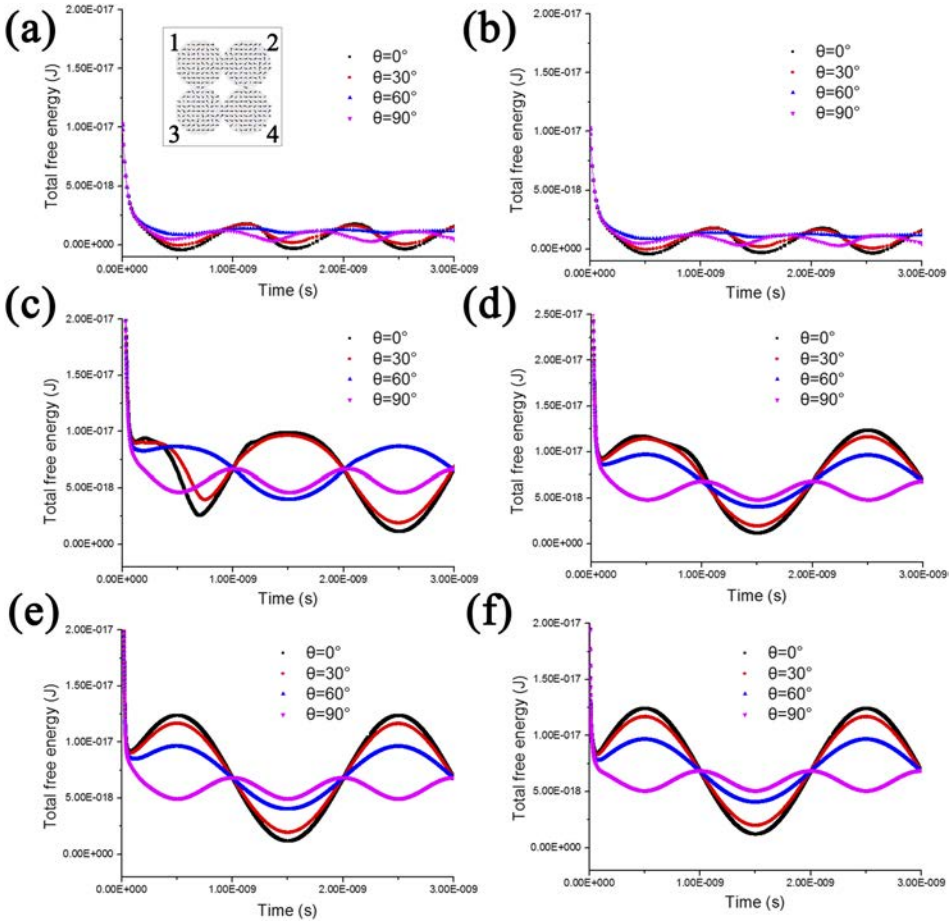

FIG. 5. Four nanoparticles energy simulated by micromagnetism finite element method, including angle between the plan of the particles and the applied alternating magnetic field at 0°, 30°, 60° and 90°. Exchange coupling constant between four particles set as ($A_{12}(Fe_3O_4)$=$A_{31}(Fe_3O_4)$=$A_{34}(Fe_3O_4)$=$A_{24}(Fe_3O_4)$ and $A_{41}(Fe_3O_4)$=$A_{23}(Fe_3O_4)$); a) 0 (J/m) and 0 (J/m). b) 1.9×10^{-20} (J/m) and 1.6×10^{-20} (J/m). c) 1.9×10^{-13} (J/m) and 1.6×10^{-13} (J/m). d) 1.9×10^{-12} (J/m) and 1.6×10^{-12} (J/m). e) 1.9×10^{-11} (J/m) and 1.6×10^{-11} (J/m). f) 1.9×10^{-10} (J/m) and 1.6×10^{-10} (J/m).

coercivity of the bulk magnetic material was regarded as the residual magnetization. The disk-like bulk magnet was commercially available. Based on the product description, the chemical composition is Sr-doping ferrite. The disk-like bulk magnet actually was different from the LBL-assembled film of Fe_3O_4 nanoparticles in magnetic microstructure. For the disk-like bulk magnet, the magnetic microstructure was multi-domains. The small magnetic moments were coupled into unanimous orientation to form magnetic domains by the quantum exchanging interaction. The material was magnetized by the rotation of domains and the displacement of domain walls. Due to the anisotropic energy, the magnetic domains were incapable of reverting into the original state after the external magnetic field was removed. For the LBL-assembled film of Fe_3O_4 nanoparticles, one nanoparticle can be regarded as a small magnetic moment due to the extremely small size, which was disturbed into random orientation by thermal fluctuation. The coupling of magnetic moments in the LBL-assembled film of nanoparticles was mainly through the magnetic dipolar interaction. The different magnetic microstructures mean it will need different strength of external magnetic field to make the bulk disk-like magnet and the LBL-assembled film of magnetic nanoparticles into the magnetic disordered state after they are magnetized. Because the magnetic dipolar interaction is much weaker than the quantum exchanging interaction, the strength of external magnetic field will be much higher for the disk-like bulk magnet than that for the magnetic LBL-assembled film. The simulated hysteresis loops of a magnetic film without and with the residual magnetization were shown in the supplementary material, Fig. S6a, b. The residual magnetization changed the magnetism of the film from superparamagnetism

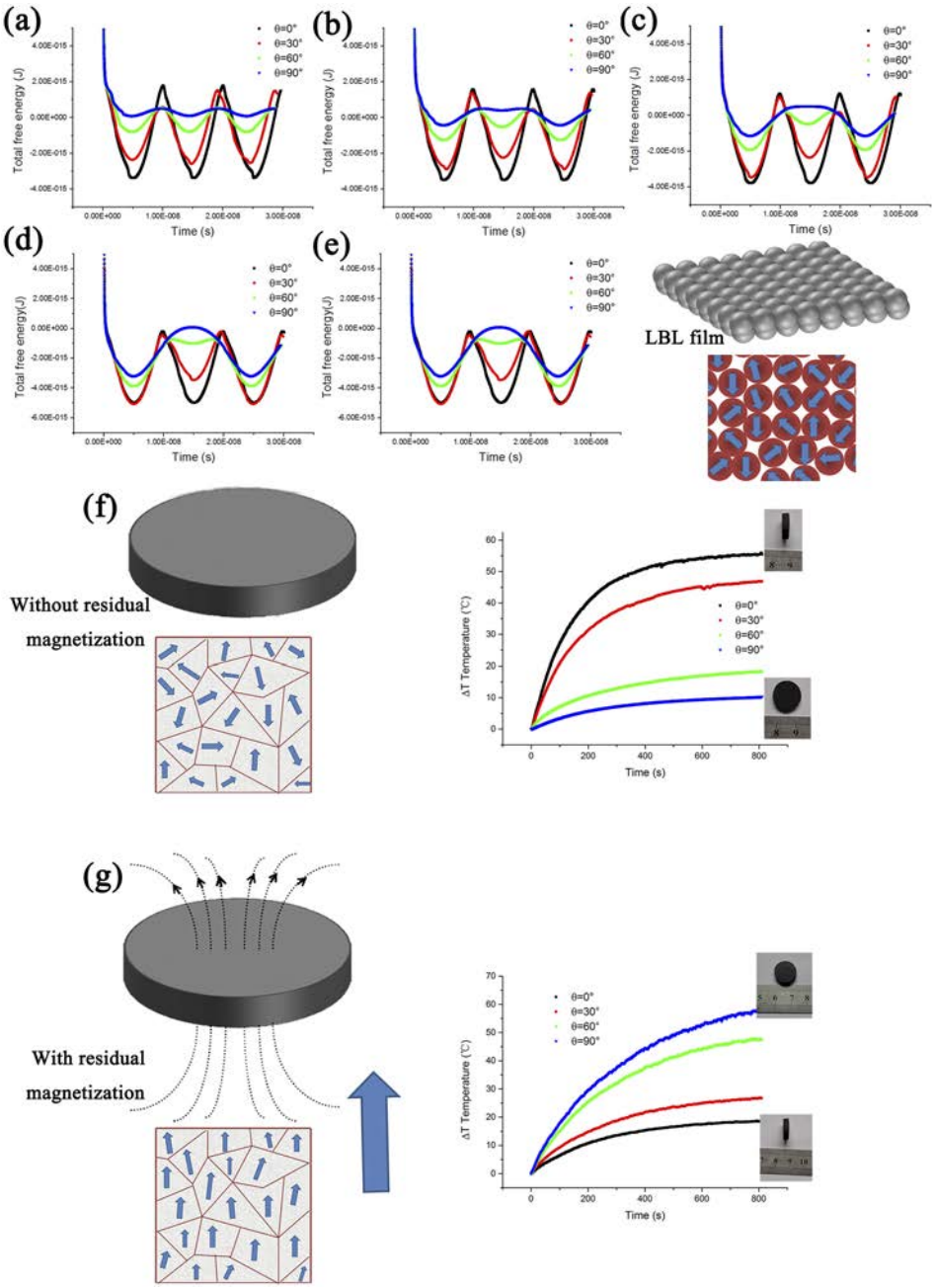

FIG. 6. Micromagnetic simulation of energy change with alternating fields (20 mT). a) The intrinsic magnetic strength of the film is 0 mT. b) The intrinsic magnetic strength of the film is 10 mT. c) The intrinsic magnetic strength of the film is 20 mT.d) The intrinsic magnetic strength of the film is 40 mT. e) The intrinsic magnetic strength of the film is 60 mT. f) Conceptual scheme of the intrinsic magnetic order for the LBL assembled film and maghemite disk material with residual magnetic field. g) The magnetothermal measurement of the maghemite disk material with residual magnetic field under the alternating magnetic field.

to ferromagnetism. This transition can be interpreted using the so-called "molecular field theory",[29,30] where the residual magnetization played a role like coupling between the magnetic moments of electrons. Magnetization (M-H) curves of the LBL-assembled film of Fe_3O_4 nanoparticles and the bulk disk-like magnet were measured by Vibrating Sample Magnetometer (VSM), which exhibited the identical results with those simulated with the OOMMF program (supplementary material, Fig S6c, d) so that the two materials may be able to act as the antithetical models. Here it should be mentioned

that all the measurements of M-H curves were done at room temperature (above 293K), which will make the dipolar couplings of magnetic nanoparticles facile to break under the turbulency of thermal energy. It was found that the coercivity of disk-like bulk magnet was much larger than that of the LBL-assembled film of nanoparticles. This was in accordance with the above-mentioned analysis. Because the ferrite was used as the permanent magnet, it should be magnetized to maximize the remanence so that there was strong interaction between the domains (For the magnet in our experiments, the remanence was about 100mT). Thus, it will need a much stronger external magnetic field to destroy the magnetic order. This means the coercivity of the ferrite disk is much larger than that of the LBL-assembled film. The thermogenic measurements of the without and with the intrinsic magnetic maghemite disk are shown in Fig 6f, g. Here, the remenance was approximately 100mT, far above the intensity of the external alternating magnetic field (20mT). The results indicate that the magnetothermal anisotropy was truly reversed by the internal magnetization, partly proving our hypothesis concerning the LBL-assembled film of nanoparticles based on the simulation. The result that the magnetothermal anisotropy can be reversed by the internal magnetization demonstrated that the magnetothermal anisotropy of assembled magnetic nanoparticles is not only dependent upon the magnetic Gibb's free energy but also can be modulated by the intrinsic magnetization state.

CONCLUSIONS

In summary, it was confirmed that the thermogenesis of a LBL-assembled film of Fe_3O_4 nanoparticles was anisotropic and was maximized when the external alternating magnetic field was parallel to the film. By simulation and experiments, this phenomenon was analyzed from the viewpoint of magnetic free energy and the interaction between nanoparticles was thought to play an important role in this process. Furthermore, the intrinsic magnetization state was found to be capable of reversing this magnetothermal anisotropy. Our results suggest that the magnetothermal effect for an assembled film of magnetic nanoparticles can be tailored not only by the interaction between elemental units but also by the intrinsic magnetization state of the system. This conclusion will enrich the controllability of the magnetothermal effect for magnetic nanoparticles in practice.

EXPERIMENTAL

Nanoparticles synthesized and LBL assembly

Fe_3O_4 nanoparticles were synthesized by co-precipitation method. Firstly, 25% (w/w) $N(CH_3)_4OH$ was slowly added to a mixture of $FeCl_2{\bullet}4H_2O$ and $FeCl_3{\bullet}6H_2O$ (the molar ratio was 1:2) that was dissolved in 2.5 mL of ultrapure water until the pH value reached 13. Then 1.5 mL of ammonium hydroxide was added into the mixture. The solution was heated to 70°C for half an hour with strong stirring during this process. After the colloidal suspension was cooled down to room temperature, the nanoparticles were washed for three times with ultrapure water and magnetically separated repeatedly. LBL assembly of nanoparticles was performed on a glass substrate.[31] The glass disks (diameter: 2.5cm) were cleaned with a mixture of H_2O_2/H_2SO_4 (volume ratio was 1:3) at boiling temperature. Then the glass disks were dipped into a 20%wt poly-dimethyldiallylammonium chloride (PDDA, molecular weight: ~100000-200000) solution for 10min. Then, the glass disks were dried by N_2 stream after washing with ultrapure water to remove the un-adsorbed polymer molecules. After that, the glass disks were dipped into the Fe_3O_4 colloidal suspension for 15min to form a layer of nanoparticles and the glass disks were likewise dried by N_2 stream after washing with ultrapure water to remove the un-adsorbed nanoparticles. A multi-layered film of nanoparticles can be fabricated by repeating this process.

Micromagnetism method

The dynamics of magnetic moments was studied by numerical simulation of the Landau-Lifshitz-Gilbert (LLG) differential equation which can be expressed as

$$\frac{d\vec{M}}{dt} = -|\gamma|\,\vec{M}\times\vec{H}_{eff} - \frac{|\gamma|}{M_s}\vec{M}\times\left(\vec{M}\times\vec{H}_{eff}\right)$$

where H_{eff} is the effective field representing all forces acting on the magnetic moment, γ is the gyromagnetic ratio, α is the damping constant, M is the magnetic moment and M_s is the saturated value of M.[32] Here, the magnetic nanoparticles were simulated with the finite difference method with various angles (0°, 30°, 60° and 90°) between the particles and the alternating magnetic field (400 KHz). The magnetic particles diameter were set as 10 nm. The dipole-dipole energy,[33–35] U_{dd}, is simply the work from infinity to a finite separation,[2] $\boldsymbol{r}$.

$$U_{dd} = \frac{\vec{m}_1 \cdot \vec{m}_2 - 3(\vec{m}_1 \cdot \hat{r})(\vec{m}_2 \cdot \hat{r})}{4\pi\mu_0 r^3}$$

For two dipoles with moments ($\vec{m}_1$) and ($\vec{m}_2$). For "in line" dipoles, the interaction is attractive with a magnitude $-m^2/2\pi\mu_0 r^2$. For Fe_3O_4 with a magnetic saturation of $Ms = 4.8\times10^5 Am^{-1}$, the characteristic dipole-dipole energy for a 10nm particle is 1.9×10^{-20}J at room temperature. The exchange constant can be estimated to be 1.9×10^{-12}J/m. In the process of assembly, the particles will aggregate to a certain extent. The dipole-dipole energy for a 200nm particle is 7.6×10^{-18} J. For system of four nanoparticles, we set the exchanging interaction between particles with different exchanging constants ($A_{12}(Fe_3O_4)=A_{31}(Fe_3O_4)=A_{34}(Fe_3O_4) = A_{24}(Fe_3O_4)$ and $A_{41}(Fe_3O_4) = A_{23}(Fe_3O_4)$). For system of nine nanoparticles, we set the exchange interaction between particles likewise.

SUPPLEMENTARY MATERIAL

See supplementary material for hydrodynamic size and ζ potential of the synthesized colloidal Fe_3O_4 nanoparticles, XRD characterization of the LBL-assembled film of nanoparticles, magnetothermal mappings of the LBL-assembled film in different orientations and simulations about the dynamics of magnetic moments, magnetic energy and hysteresis loop of magnetic film.

ACKNOWLEDGMENTS

This work was supported by the National Basic Research Program of China (2013CB733801) and the National Key Research and Development Program of China (2017YFA0104301). J. Liu is thankful to the National Science Foundation of China (11574246). J. Sun is thankful to the Fundamental Research Funds for the Central Universities. F. Fan, J. Sun, S. Ma and N. Gu appreciate the supports from Collaborative Innovation Center of Suzhou NanoScience and Technology.

[1] R. Hergt, S. Dutz, R. Müller, and M. Zeisberger, J Phys-Condens Matter **18**, 2919 (2006).
[2] A. Espinosa, R. D. Corato, J. Kolosnjajtabi, P. Flaud, T. Pellegrino, and C. Wilhelm, ACS Nano **10**, 2436 (2016).
[3] C. Guibert, V. Dupuis, V. Peyre, and J. Fresnais, J. Phys Chem C **5**, 4224 (2015).
[4] V. Raeesi, L. Y. T. Chou, and W. C. W. Chan, Adv Mater **28**, 8511 (2016).
[5] R. Gangemi, L. Paleari, A. M. Orengo, A. Cesario, L. Chessa, S. Ferrini, and P. Russo, Curr Med Chem **16**, 1688 (2009).
[6] P. Tseng, J. W. Judy, and C. D. Di, Nat Methods **9**, 1113 (2012).
[7] L. Robledo, J. Elzerman, G. Jundt, M. Atatüre, A. Högele, S. Fält, and A. Imamoglu, Science **320**, 772 (2008).
[8] Z. Wu, T. Si, W. Gao, X. Lin, J. Wang, and Q. He, Small **12**, 550 (2016).
[9] S. Laurent, D. Forge, M. Port, A. Roch, C. Robic, E. L. Vander, and R. N. Muller, Chem Rev **39**, 2064 (2008).
[10] Q. Wang, B. Chen, F. Ma, S. Lin, M. Cao, Y. Li, and N. Gu, Nano Res **10**, 626 (2016).
[11] M. Arsianti, M. Lim, C. P. Marquis, and R. Amal, Biomacromolecules **11**, 2521 (2010).
[12] S. Laurent, S. Dutz, U. O. Hafeli, and M. Mahmoudi, Adv Colloid Interface Sci **166**, 8 (2011).
[13] A. Espinosa, R. D. Corato, J. Kolosnjajtabi, P. Flaud, T. Pellegrino, and C. Wilhelm, ACS Nano **10**, 2436 (2016).
[14] S. Kralj and D. Makovec, ACS Nano **9**, 9700 (2015).
[15] K. Hu, J. Sun, Z. Guo, P. Wang, Q. Chen, M. Ma, and N. Gu, Adv. Mater. **27**, 2507 (2015).
[16] J. Sun, X. Liu, J. Huang, L. Song, Z. Chen, H. Liu, Y. Li, Y. Zhang, and N. Gu, Sci Rep **4**, 5125 (2014).
[17] X. Liu, J. Zhang, S. Tang, J. Sun, Z. Lou, Y. Yang, P. Wang, Y. Li, and N. Gu, Science China Mater **59**, 901 (2016).
[18] J. Sun, F. Fan, P. Wang, S. Ma, L. Song, and N. Gu, ChemPhysChem **17**, 3377 (2016).
[19] C. L. Hu, Y. C. Zhou, L. Liao, and R. L. Stamps, J Magn Magn Mater **386**, 146 (2015).
[20] M. Ali, P. Adie, C. H. Marrows, D. Greig, B. J. Hickey, and R. L. Stamps, Nat Mater **6**, 70 (2007).
[21] D. Soto-Aquino and C. Rinaldi, J Magn Magn Mater **393**, 46 (2015).
[22] V. L. Zhang, C. G. Hou, K. Di, H. S. Lim, S. C. Ng, S. D. Pollard, H. Yang, and H. K. Meng, AIP Advances **7**, 055212 (2017).
[23] Y. Li, K. Hu, B. Chen, Y. Liang, F. Fan, J. Sun, Y. Zhang, and N. Gu, Colloids and Surfaces A **520**, 348 (2017).
[24] S. Sun and H. Zeng, J. Am. Chem. Soc. **124**, 8204 (2002).
[25] M. Ma, Y. Zhang, W. Yu, H.-Y. Shen, H.-Q. Zhang, and N. Gu, Colloids and Surfaces A **212**, 219 (2003).
[26] P. Wang, J. Sun, Z. Lou, F. Fan, K. Hu, Y. Sun, and N. Gu, Adv. Mater. **28**, 10801 (2016).

[27] C. Guibert, V. Dupuis, V. Peyre, and J. Fresnais, J. Phys. Chem. C **5**, 4224 (2015).
[28] B. Bharti, A. L. Fameau, M. Rubinstein, and O. D. Velev, Nat. Mater. **14**, 1104 (2015).
[29] S. I. Ohkoshi and Y. Abe, Phys. Rev. Lett. **82**, 1285 (1999).
[30] J. M. Rodgers, C. Kaur, Y. G. Chen, and J. D. Weeks, Phys. Rev. Lett. **97**, 0907801 (2006).
[31] Z. Tang, Y. Wang, P. Podsiadlo, and N. A. Kotov, Adv. Mater. **18**, 3203 (2007).
[32] E. Olive, Y. Lansac, M. Meyer, M. Hayoun, and J.-E. Wegrowe, J. Appl. Phys. **117**, 213904 (2015).
[33] M. Grzelczak, J. Vermant, E. M. Furst, and L. M. Lizmarzán, ACS Nano **4**, 3591 (2010).
[34] A. F. Demirors, P. P. Pillai, B. Kowalczyk, and B. A. Grzybowski, Nature **503**, 99 (2013).
[35] K. J. Bishop, C. E. Wilmer, S. Soh, and B. A. Grzybowski, Small. **5**, 1601 (2009).